SUPPLEMENTAL MATERIALS AND METHODS

Protein Expression and Purification – All constructs were expressed in *Escherichia Coli* BL21(DE3) star cells (Invitrogen). Cells were grown at 250 rpm and 37°C. Cultures were induced at OD_{600nm} of ~0.5-0.6 with isopropyl-1-thio-β-D-galactopyranoside at a final concentration of 0.2 mM. $GAFA_{125-320}$, $GAFA_{154-320}$ or $GAFB_{332-496}$ were grown for 22 hours at 22°C after induction, while $GAFAB_{134-496}$ and $GAFAB_{154-496}$ were grown for 22 hours at 16°C after induction. For NMR experiments, proteins were expressed in M9 minimal medium, modified accordingly with [^{15}N]-NH_4Cl, [^{13}C]-Glucose and/or 99% D_2O (Cambridge Isotope Laboratories). Cells were harvested through centrifugation and lysed by a microfluidizer (M110EH, Microfluidics International). The purification was performed at 4°C. $GAFAB_{134-496}$, $GAFAB_{154-496}$ and $GAFB_{332-496}$ were purified from the soluble fraction by nickel affinity chromatography, whereas $GAFA_{125-320}$ and $GAFA_{154-320}$ were re-solubilized into 6M Gu-HCl and refolded in the presence of cGMP through stepwise decrease of Gu-HCl concentrations while bound to immobilized and Ni^{2+}-bound iminodiacedic acid (Sigma). Upon elution, DTT was added to a final concentration of 1 mM. The nickel column eluant was concentrated with Amicon Ultra-15 (10 kDa cut-off) to < 2 ml and injected onto a Superdex-75 or Superdex-200 size exclusion column (Amersham). Proteins were eluted with NMR buffer (150 mM NaCl, 25 mM sodium phosphate pH 7.0, 0.1 mM EDTA). Upon fractionation, DTT to a final concentration of 1 mM was added. The purity of the fractions was assessed by SDS-PAGE and fractions were pooled accordingly. For NMR experiments, the pooled fractions were concentrated with Amicon Ultra-4 (10 kDa cut-off) to 0.5 – 1.5 mM. $GAFA_{154-320}$ could be lyophilized and stored over several months without loss of structural integrity, as determined by NMR.

Determination of Stokes' Radius – The Stokes' radii of the PDE5 constructs were determined by size exclusion chromatography (Superdex-200 column, 1.0 x 86.0 cm, Amersham) at 25ºC. Samples contained 0.4 mM of purified $GAFA_{154-320}$, $GAFA_{125-320}$, $GAFB_{332-496}$, $GAFAB_{134-496}$, or $GAFAB_{154-496}$ and were run in triplicate. The size exclusion chromatography column was standardized with protein of known Stokes' radii: alcohol dehydrogenase (45.5 Å), bovine serum albumin (36.0 ± 0.9 Å), carbonic anhydrase (21.4 ± 1.8 Å), and cytochrome c (17.5 ± 1.1 Å) (Sigma). Stokes' radii of the standard proteins are the average of previously published values (1-6). Errors indicate standard deviation. Elution position of protein standards (n = 2) were used to generate a standard curve of Stokes' radius versus $(-\log K_{av})^{1/2}$ that was used to calculate the Stokes' radii of PDE5 constructs. The distribution coefficient K_{av} was determined from the elution volume (V_e), void volume (V_0) and inclusion volume (V_i) according to equation 1:

$$K_{av} = \frac{V_e - V_0}{V_i - V_0}$$

Determination of Sedimentation Coefficient – Sedimentation coefficients of PDE5 constructs at NMR concentrations were determined by sedimentation velocity of the PDE5 constructs at 40,000 rpm and 25°C using a Beckman XL-A analytical ultracentrifuge. Radial scans were acquired at 295 nm for ~10 h. Data analysis was performed using the continuous c(s) distribution model and independent species model features in SedFit v10.3 (7). The molecular mass of each PDE5 construct was calculated using the Siegel and Monty equation (8) as previously described (1). Predicted molecular weight based on the amino acid sequence was calculated using the ProtParam tool (9).

H-D exchange experiments – Lyophilized uniformly [^{15}N]-labeled $GAFA_{154-320}$ was resuspended in 99.9% D_2O and a series of short [^{1}H,^{15}N]-HSQC spectra (~17 minutes) was collected immediately on a Bruker 500 MHz DMX spectrometer with a triple-resonance cryoprobe at 37ºC to monitor exchange of amide protons with solvent via disappearance of the proton signal over time for up to several days. After ~5 days, a final [^{1}H,^{15}N]-HSQC spectrum was collected on a Varian INOVA 900 MHz to identify the slowest exchanging and solvent-protected amide resonances.

Determination of the rotational correlation time – To determine the rotational correlation time τ_c of $GAFA_{154-320}$ in the presence of cGMP, we measured ^{15}N-spin relaxation parameters (R_1, R_2) using standard pulse sequences (10) at 37˚C on a Bruker 500 MHz DMX spectrometer. [^{15}N]-T_1 relaxation delays were 10, 50, 100, 200, 400, 600, 800, 1000 ms (underlined delays were duplicated). [^{15}N]-T_2 relaxation delays were 17.2, 34.4, 51.7, 69.0, 86.2, 103.5, 120.7 ms (underlined delays were duplicated). The average ratio of T1/T2 was used to calculate τ_c by the *r2r1_diffusion* program (11).

[^{3}H]-cNMP filter binding assay – To determine binding of cGMP or cAMP, 0.5 µM purified protein was incubated with 1 µM [^{3}H]-cGMP or [^{3}H]-cAMP in binding buffer (5 mM Tris-HCl, pH 7.5, 25 mM NaCl, 2mM EDTA, 5 µg/ml BSA) for 16 hours at 37ºC in a final volume of 50 µL. Reactions were quenched with 1 ml 3 M $(NH_4)_2SO_4$ and filtered through pre-wet HAWP filters (Millipore, pore size: 0.45 µM) and then washed twice with 1 ml 1 M $(NH_4)_2SO_4$. Competition binding assays were conducted with 1 nM protein, 2 nM [^{3}H]-cGMP and various amounts of unlabeled cGMP or cAMP in binding buffer for 1 hour on ice in a final volume of 5 ml. Reactions were quenched with 2.5 ml 3 M $(NH_4)_2SO_4$ and filtered through pre-wet Millipore HAWP filters, which then were washed twice with 2.5 ml 1 M $(NH_4)_2SO_4$. Filters were dissolved in 5 ml Filter-Count scintillation liquid (Perkin-Elmer) and counted in a 1600 TR scintillation counter (Packard).

SUPPLEMENTAL REFERENCES

1. Zoraghi, R., Bessay, E. P., Corbin, J. D., and Francis, S. H. (2005) *J Biol Chem* **280**(12), 12051-12063
2. Safran, M., and Leonard, J. L. (1991) *J Biol Chem* **266**(5), 3233-3238
3. Olshevskaya, E. V., Ermilov, A. N., and Dizhoor, A. M. (1999) *J Biol Chem* **274**(36), 25583-25587
4. Broadus, R. M., and Haddock, J. D. (1998) *Arch Microbiol* **170**(2), 106-112
5. Sapir, T., Eisenstein, M., Burgess, H. A., Horesh, D., Cahana, A., Aoki, J., Hattori, M., Arai, H., Inoue, K., and Reiner, O. (1999) *Eur J Biochem* **266**(3), 1011-1020
6. Sincock, P. M., Ganley, I. G., Krise, J. P., Diederichs, S., Sivars, U., O'Connor, B., Ding, L., and Pfeffer, S. R. (2003) *Traffic* **4**(1), 18-25
7. Schuck, P. (2003) *Anal Biochem* **320**(1), 104-124
8. Siegel, L. M., and Monty, K. J. (1966) *Biochim Biophys Acta* **112**(2), 346-362
9. Gasteiger E., H. C., Gattiker A., Duvaud S., Wilkins M.R., Appel R.D., Bairoch A. (2005) Protein Identification and Analysis Tools on the ExPASy Server. In: Walker, J. M. (ed). *The Proteomics Protocols Handbook*, Humana Press
10. Farrow, N. A., Muhandiram, R., Singer, A. U., Pascal, S. M., Kay, C. M., Gish, G., Shoelson, S. E., Pawson, T., Forman-Kay, J. D., and Kay, L. E. (1994) *Biochemistry* **33**(19), 5984-6003
11. Tjandra, N., Kuboniwa, H., Ren, H., and Bax, A. (1995) *Eur J Biochem* **230**(3), 1014-1024
12. Thompson, W. J., Higgins D.G., Gibson T.J. (1994) *Nucleic Acids Res* **22**(22), 4673-4680

SUPPLEMENTAL FIGURE LEGENDS

Figure S1. H-D exchange of cGMP-bound $GAFA_{154-320}$. Intensities (arbitrary units) of backbone amide peaks five days after dissolution in D_2O are plotted versus residue number (see also Fig. 1B). Secondary structure elements are indicated.

Figure S2. (A) Surface presentation of the binding pocket of PDE5A GAF A. Colors indicate relative electrostatics. Red areas are negatively polarized and blue areas are positively polarized relative to mean. In PDE5A, cGMP buries a surface area of 358.8 $Å^2$, similar to the buried surface of cGMP in PDE2A (348.2 $Å^2$) and cAMP in cyaB2 (337.5 $Å^2$). (B) The structures of cGMP-bound PDE5A GAF A (green), cGMP-bound PDE2A GAF B (yellow, 1MC0), and cAMP-bound cyaB2 GAF B (pink, 1YKD) were aligned using PyMOL (40). The cNMP molecules are displayed in sticks with carbon color according to the ribbon projection of the GAF domains. Though bound in a similar overall orientation, the cGMP molecule in PDE5A is tilted by several degrees when compared with cGMP in PDE2A and cAMP in cyaB2. Tighter hydrophobic packing of the guanine ring mainly through residues Ile211 and Ile275 is responsible for this tilt as a similar orientation as in PDE2A and cyaB2 would lead to steric clashes with their side chains. Nevertheless, it is possible that this nucleotide tilt is a consequence of the limited number of NOEs that define the guanine ring and that cGMP is oriented more similar to the nucleotides in the other GAF domains. (C) PDE2A GAF B binding pocket. Binding residues are displayed as sticks with carbon atoms in cyan. Direct intermolecular hydrogen bonds are shown as black dashed lines. (D) cyaB2 GAF B binding pocket. Binding residues are displayed as sticks with carbon atoms in cyan. Direct intermolecular hydrogen bonds are shown as black dashed lines.

Figure S3. Sequence alignment of cNMP binding GAF domains. cGMP binding mouse PDE5A GAF A, cGMP binding mouse PDE2A GAF B, cGMP binding chicken PDE6C GAF A, cAMP binding human PDE10A GAF B, cGMP binding human PDE11A GAF A, and cAMP binding cyanobacterial adenylyl cyclase cyaB2 GAF A and B. Identical residues are highlighted in red, strongly similar residues in green and weakly similar residues in blue. Alignment was performed with CLUSTALW (12). Secondary structure elements from PDE5A are indicated.

Figure S4. One-dimensional proton NMR spectra of $GAFA_{125-320}$ D196A purified without addition of cyclic nucleotide.

Figure S5. Spectral overlay of tandem GAF domains with GAF A and GAF B. (A) Key for the spectral overlay: cGMP-bound $GAFAB_{154-496}$ in black, apo-$GAFAB_{154-496}$ in red, $GAFB_{332-496}$ in blue, and cGMP-bound GAF A in green. (B) [^1H,^{15}N]-TROSY-HSQC spectral overlay of cGMP-bound PDE5 $GAFAB_{154-496}$ recorded in the absence (red) and presence (black) of cGMP with cGMP-bound $GAFA_{154-320}$ (green) and $GAFB_{332-496}$ (blue). (C) Magnification of region indicated by box in (B). (D) Magnification of region indicated by box in (B). Spectral overlay of apo $GAFAB_{154-496}$ (red) and cGMP-bound $GAFAB_{154-496}$ (black). (E) Magnification of region indicated by box in (B). Spectral overlay of apo $GAFAB_{154-496}$ (red) and $GAFB_{332-496}$ (blue). Rectangles indicate resonances that are still detectable and appear less affected by the apo-state of GAF A; circles indicate resonances that are broadened beyond detection by the apo-state of GAF A.

Figure S6. SEC profile of PDE5A $GAFA_{154-496}$ WT in 6M Gu-HCl. Absorbance at 260 nm. Data shown are representative for three independent experiments.

Figure S7. AUC and SEC of $GAFAB_{154-496}$ and $GAFAB_{134-496}$. (A) Profiles of $GAFAB_{154-496}$ (red) and $GAFAB_{134-496}$ (black). C(s) plotted vs. sedimentation coefficient. (B) SEC profiles of $GAFAB_{154-496}$ (red) and $GAFAB_{134-496}$ (black). Absorbance at 230 nm plotted versus column volume (SDX200, 1 cv = 172.9 ml). Profiles shown in (A) and (B) are representatives for triplicate experiments.

Table S1. Experimental NMR restraints and structural statistics for the structure of PDE5A GAF A bound to cGMP.

Structural restraints (residues 154-302)	
Protein NOE distance restraints	
short-range ($\|i-j\| \leq 1$)	1053
medium-range ($1< \|i-j\| < 5$)	372
long-range ($\|i-j\| \geq 5$)	738
total	2163
dihedral angles restraints	
phi	97
psi	97
hydrogen bonds	50
protein-ligand NOEs	37
total restraints	2444
restraints per residue	16.4
Ensemble RMSD (20 models)	
residues 154-302	
mean global backbone atoms	0.93 ± 0.20 Å
mean global heavy atoms	1.51 ± 0.15 Å
residues 157-277, 285-302	
mean global backbone atoms	0.53 ± 0.10 Å
mean global heavy atoms	1.31 ± 0.11 Å
Ramachandran statistics (20 models, residues 157-277, 285-302)	
most favored	86.6 %
additionally allowed	9.9 %
generously allowed	1.8 %
disallowed	1.7 %
Restraint violations	
average number of NOE violations per structure > 0.2 Å	2.2
average number of NOE violations per structure > 0.5 Å	0.0
average number of dihedral angle violations per structure > 2˚	1.3

Figure S1.

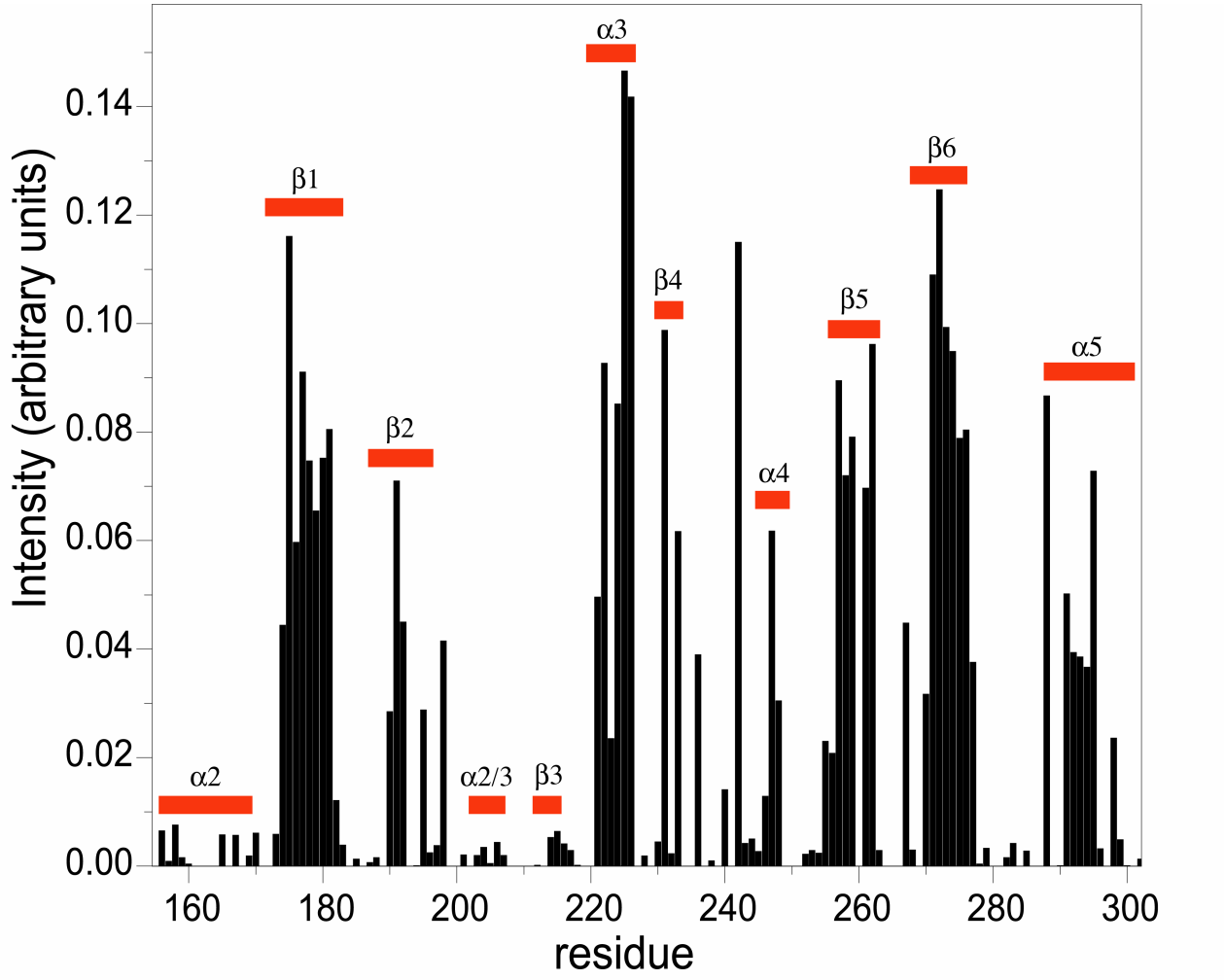
α3
β6
β1
β4
β5
α5
β2
α4
α2
α2/3
β3
Intensity (arbitrary units)
0.00
0.02
0.04
0.06
0.08
0.10
0.12
0.14
160
180
200
220
240
260
280
300
residue

Figure S2.

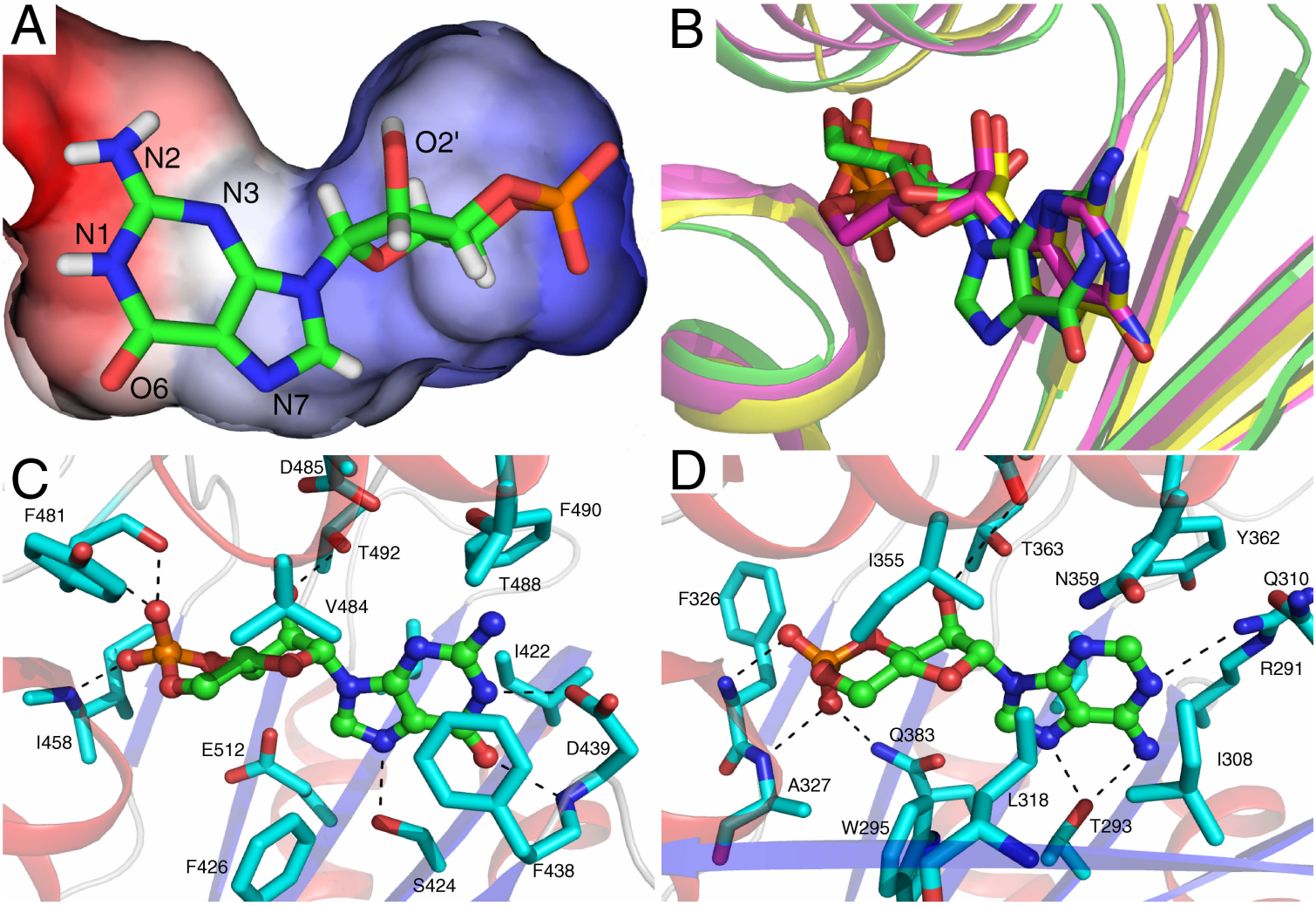
A
N2
N3
N1
O2'
O6
N7
B
C
D485
F481
F490
T492
T488
V484
I422
I458
E512
D439
F426
S424
F438
D
I355
T363
Y362
N359
Q310
F326
R291
Q383
I308
A327
L318
W295
T293

Figure S3.

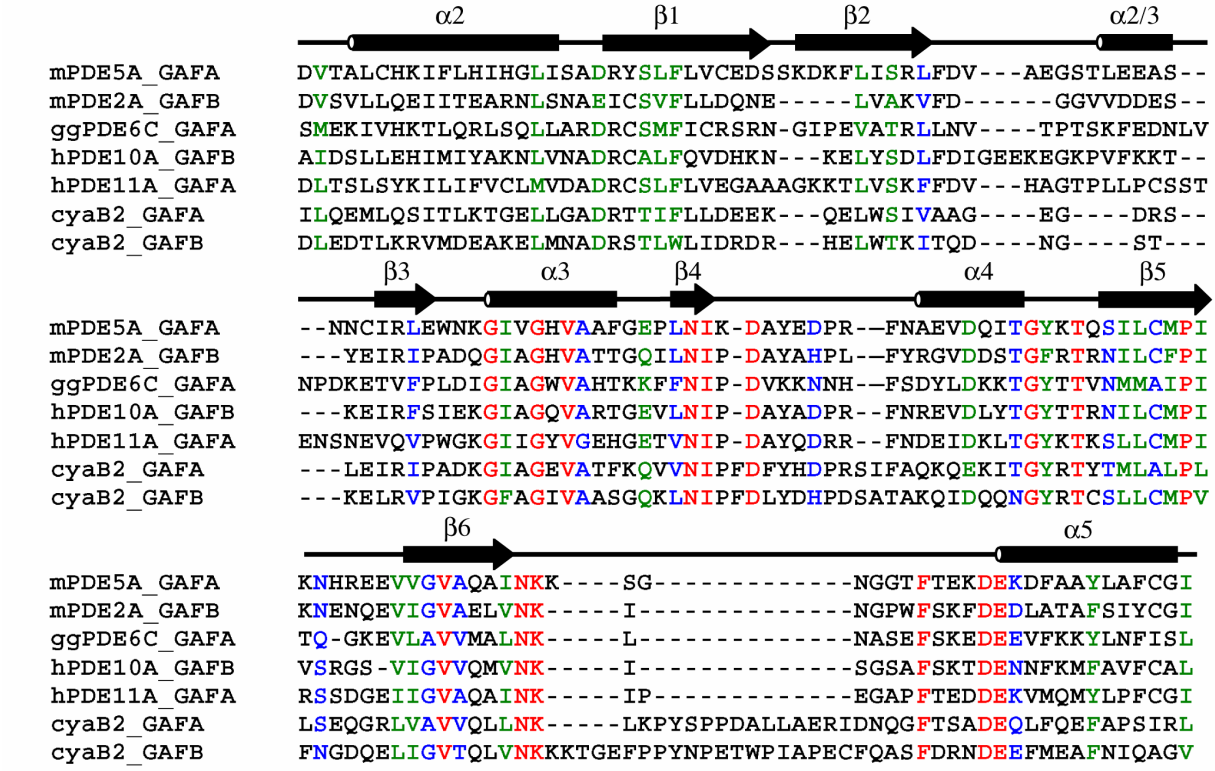
α2 β1 β2 α2/3
mPDE5A_GAFA DVTALCHKIFLHIHGLISADRYSLFLVCEDSSKDKFLISRLFDV---AEGSTLEEAS--
mPDE2A_GAFB DVSVLLQEIITEARNLSNAEICSVFLLDQNE-----LVAKVFD------GGVVDDES--
ggPDE6C_GAFA SMEKIVHKTLQRLSQLLARDRCSMFICRSRN-GIPEVATRLLNV----TPTSKFEDNLV
hPDE10A_GAFB AIDSLLEHIMIYAKNLVNADRCALFQVDHKN---KELYSDLFDIGEEKEGKPVFKKT--
hPDE11A_GAFA DLTSLSYKILIFVCLMVDADRCSLFLVEGAAAGKKTLVSKFFDV---HAGTPLLPCSST
cyaB2_GAFA ILQEMLQSITLKTGELLGADRTTIFLLDEEK---QELWSIVAAG----EG----DRS--
cyaB2_GAFB DLEDTLKRVMDEAKELMNADRSTLWLIDRDR---HELWTKITQD----NG----ST---
β3 α3 β4 α4 β5
mPDE5A_GAFA --NNCIRLEWNKGIVGHVAAFGEPLNIK-DAYEDPR--FNAEVDQITGYKTQSILCMPI
mPDE2A_GAFB ---YEIRIPADQGIAGHVATTGQILNIP-DAYAHPL--FYRGVDDSTGFRTRNILCFPI
ggPDE6C_GAFA NPDKETVFPLDIGIAGWVAHTKKFFNIP-DVKKNNH--FSDYLDKKTGYTTVNMMAIPI
hPDE10A_GAFB ---KEIRFSIEKGIAGQVARTGEVLNIP-DAYADPR--FNREVDLYTGYTTRNILCMPI
hPDE11A_GAFA ENSNEVQVPWGKGIIGYVGEHGETVNIP-DAYQDRR--FNDEIDKLTGYKTKSLLCMPI
cyaB2_GAFA ---LEIRIPADKGIAGEVATFKQVVNIPFDFYHDPRSIFAQKQEKITGYRTYTMLALPL
cyaB2_GAFB ---KELRVPIGKGFAGIVAASGQKLNIPFDLYDHPDSATAKQIDQQNGYRTCSLLCMPV
β6 α5
mPDE5A_GAFA KNHREEVVGVAQAINKK----SG-----------NGGTFTEKDEKDFAAYLAFCGI
mPDE2A_GAFB KNENQEVIGVAELVNK-----I-----------NGPWFSKFDEDLATAFSIYCGI
ggPDE6C_GAFA TQ-GKEVLAVVMALNK-----L-----------NASEFSKEDEEVFKKYLNFISL
hPDE10A_GAFB VSRGS-VIGVVQMVNK-----I-----------SGSAFSKTDENNFKMFAVFCAL
hPDE11A_GAFA RSSDGEIIGVAQAINK-----IP----------EGAPFTEDDEKVMQMYLPFCGI
cyaB2_GAFA LSEQGRLVAVVQLLNK-----LKPYSPPDALLAERIDNQGFTSADEQLFQEFAPSIRL
cyaB2_GAFB FNGDQELIGVTQLVNKKKTGEFPPYNPETWPIAPECFQASFDRNDEEFMEAFNIQAGV

Figure S4.

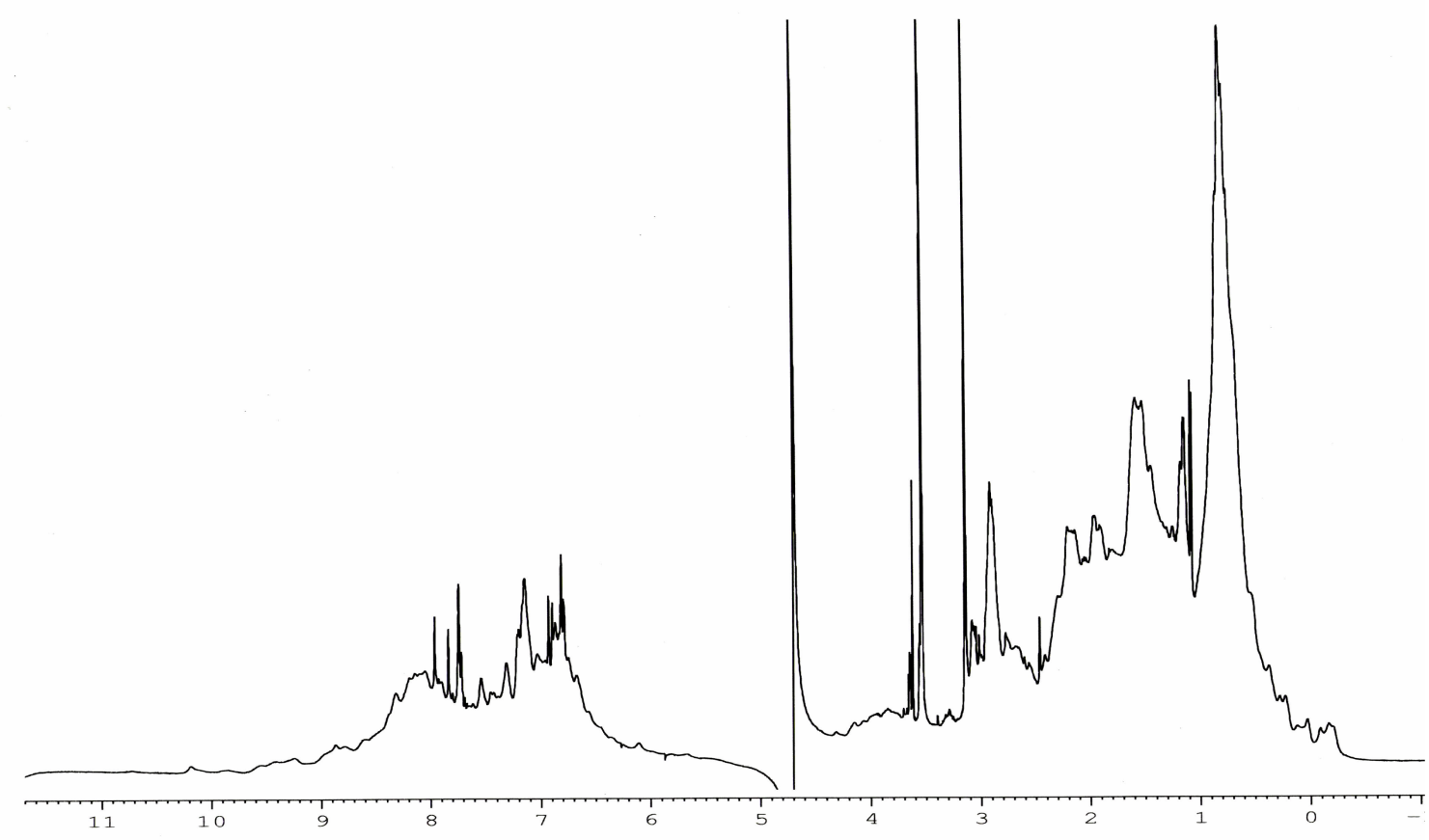

Figure S5.

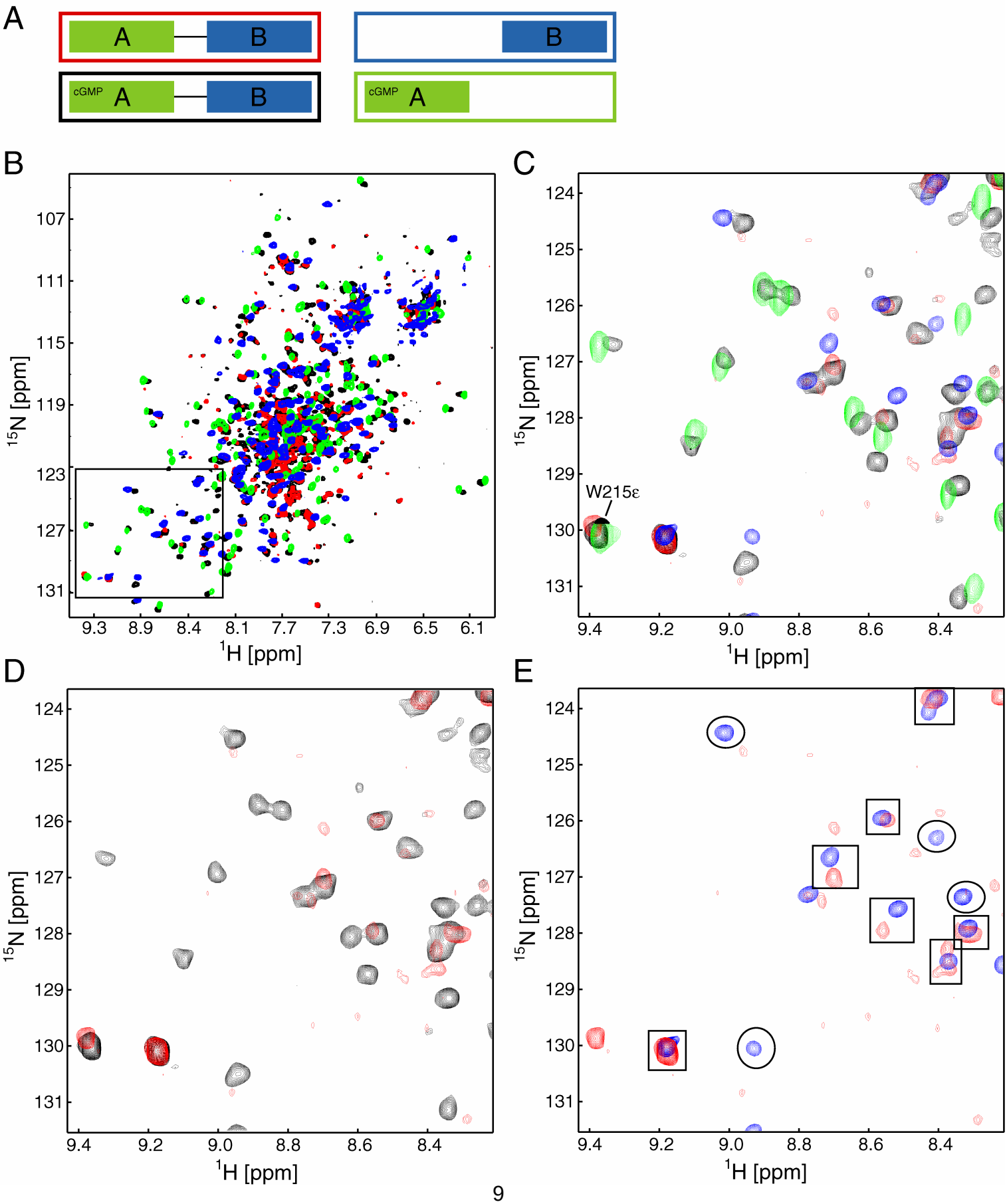
A
A
B
B
cGMP
A
B
cGMP
A
B
107
111
115
119
123
127
131
^{15}N [ppm]
9.3
8.9
8.4
8.1
7.7
7.3
6.9
6.5
6.1
^{1}H [ppm]
C
124
125
126
127
128
129
130
131
^{15}N [ppm]
W215ε
9.4
9.2
9.0
8.8
8.6
8.4
^{1}H [ppm]
D
124
125
126
127
128
129
130
131
^{15}N [ppm]
9.4
9.2
9.0
8.8
8.6
8.4
^{1}H [ppm]
E
124
125
126
127
128
129
130
131
^{15}N [ppm]
9.4
9.2
9.0
8.8
8.6
8.4
^{1}H [ppm]

Figure S6.

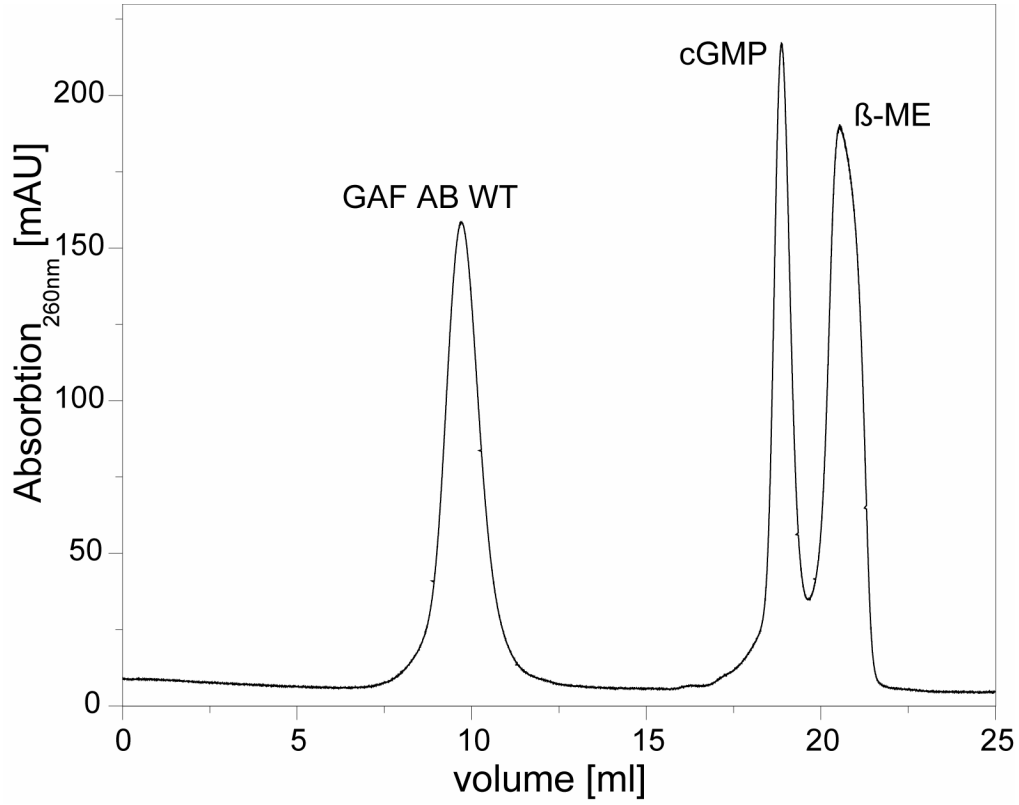
cGMP
ß-ME
GAF AB WT
Absorbtion260nm [mAU]
200
150
100
50
0
0
5
10
15
20
25
volume [ml]

Figure S7.

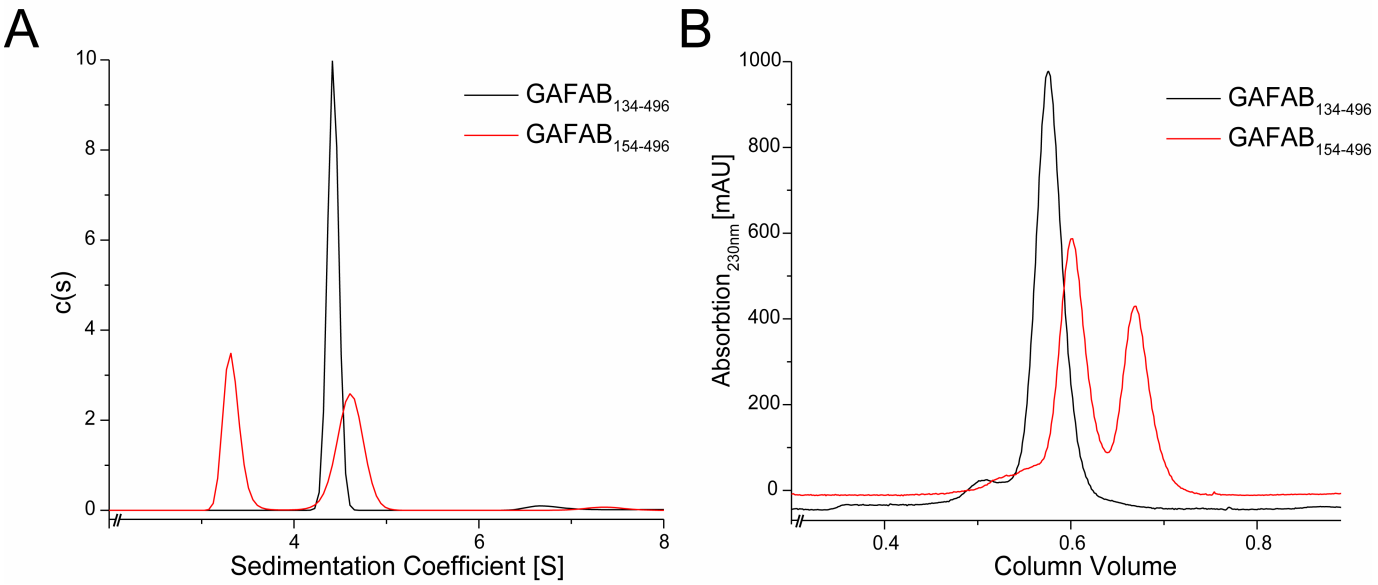
A
B
c(s)
Sedimentation Coefficient [S]
GAFAB134-496
GAFAB154-496
Absorbtion230nm [mAU]
Column Volume